Band gaps and defect modes in periodically structured waveguides

J. N. Munday, C. Brad Bennett, and W. M. Robertson[a)]
Department of Physics and Astronomy, Middle Tennessee State University, Murfreesboro, Tennessee 37132

(Received 7 August 2001; revised 28 May 2002; accepted 1 June 2002)

This work examines a simple one-dimensional acoustic band gap system made from a diameter-modulated waveguide. Experimental and theoretical results are presented on perfectly periodic waveguide arrays showing the presence of band gaps—frequency intervals in which the transmission of sound is forbidden. The introduction of defects in the perfect periodicity leads to narrow frequency transmission bands—defect states—within the forbidden band gaps. The circular cross-section waveguide system is straightforward to simulate theoretically and experimental results demonstrate good agreement with theory. The experimental transmission of the periodic waveguide arrays is measured using an impulse response technique. © *2002 Acoustical Society of America.*
[DOI: 10.1121/1.1497625]

PACS numbers: 43.28.Bj, 43.28.Dm, 43.25.Ts [LLT]

I. INTRODUCTION

In this paper the properties of acoustic band gaps and defect modes in periodically structured waveguides are examined theoretically and experimentally. There has been considerable recent interest in the propagation of classical waves—electromagnetic and acoustic—in periodically structured environments. The goal of much of this research is to design and create composite materials—so-called photonic or acoustic band gap arrays—that can manipulate the properties of the radiation field. In the electromagnetic case the ability to engineer light has led to the suggestion and/or development of a number of important applications.[1–4] Similar practical applications for acoustic waves have been suggested[5–7] although research in this area is far less extensive.

Many of the projected applications of acoustic and photonic band gap materials require composite systems with forbidden transmission in all three spatial dimensions—so-called complete band gap materials. In practice such materials are difficult to realize because they require a three-dimensional periodic composite between two materials with considerably different impedances. As a consequence much work has focused on band gap phenomena in systems with periodicity, and hence band gaps, in two[8,9] or one dimensions.[10,11] Studies of lower dimensional systems are conducted as analogs of three-dimensional systems and for applications in their own right. In the work described here we reexamine a one-dimensional periodic waveguide system that has received considerable theoretical and experimental attention.[12–16] The specific emphasis in this work is the examination of defect modes created when the perfect periodicity is broken. Defect modes are an essential ingredient in many of the proposed applications of photonic or acoustic band gap systems. Although the properties of periodic acoustic waveguides have been long studied, little attention has been given to the properties of defect modes.

The basis of acoustic band gap effects rests on the fact that in a perfectly periodic composite system consisting of two materials with significantly different acoustic impedances, the coherent effects of scattering and interference lead to frequency intervals in which propagation of sound is forbidden—so-called acoustic or sonic band gaps. Because of the close analogy of this process to the scattering and interference of electron wave functions by the periodic potential of a crystalline lattice, much of the terminology and theoretical methods of solid state physics have been adopted in the treatment of acoustic (and electromagnetic) band gap phenomena. A key success of solid state physics was the unfolding of the role of the electron state band gap in explaining and understanding the properties of semiconductors. However, an essential step in going from an understanding of the properties of perfectly crystalline semiconductors to practical devices involved the addition of defects. Small quantities of donor or acceptor defect atoms were found to perturb the perfect lattice and create isolated electron states within the forbidden band gap. A similar sequence is adopted in the work described here. We first examine a perfectly periodically structured acoustic waveguide system and show the existence of forbidden transmission bands. The periodic system consists of a series of equal length segments of circular cross-section waveguides with diameters varying between two different values. Next, we introduce a single defect in the perfect periodicity, and we show that this defect produces a narrow band of transmission within the previously forbidden band gap. The defect is produced by altering the length of the central segment of the series of waveguides. Depending on the precise nature of the defect we observe either donor-like or acceptor-like behavior.

There are many methods to calculate the acoustic response of a one-dimensional waveguide.[13,15] In the work described here, an iterative theoretical formalism is adapted from Fresnel's equations to calculate the reflection and transmission of the periodic waveguide system. The theoretical calculations show that it should be possible to produce extremely narrow band filters using defects in this simple

a)Electronic mail: wmr@physics.mstu.edu

waveguide configuration. We demonstrate that although it is possible to produce narrow band filters, the extremely narrow theoretical predictions are not realized in practice. We discuss the experimental limitations that do not allow us to realize the narrowest filters and explain the steps that could be taken to circumvent these limitations.

II. THEORY

The experimental system that we chose to investigate in this work consisted of a waveguide of circular cross section with a diameter that was modulated periodically between a small and large diameter as a function of length. The waveguide dimensions and the frequency interval explored were selected so that our measurements were all conducted in the lowest transverse mode of the waveguide. This criterion was assured by using frequencies below the cutoff frequency, f_c, of the next higher transverse mode given by[17,18]

$$f_c = 0.92\frac{c}{\pi a},$$

where c is the speed of sound and a the larger tube diameter. Furthermore, the lengths of the waveguide sections were chosen to be much larger than the diameter of the largest tube so that the stop band phenomena observed in our experiments were due to interference in the longitudinal direction and not due to radial resonances in the waveguide segments themselves. The cavity resonance effect will occur at frequencies well above those used in our experiments here.

A detailed description of the exact waveguide parameters used in the measurements and in the associated theoretical calculations is given in the following experimental description. The reflection and transmission of the periodically diameter-modulated waveguide system can be easily modeled theoretically. The different diameter waveguides have different acoustic impedance values, Z. In the long wavelength approximation, Z is given by the simple expression[19]

$$Z = \frac{\rho c}{S},$$

where ρ is the density of air, and S is the cross-sectional area of the waveguide. Provided that the long wavelength condition is met, the impedance is independent of frequency. The amplitude reflection coefficient, r_{ij}, at the junction between two waveguide sections with different impedances is given by[19]

$$r_{ij} = \frac{Z_i - Z_j}{Z_i + Z_j}.$$

To extend the theoretical reflection expression to include a second boundary at a distance, d, from the first, the effects of multiple reflection and interference must be taken into account. The corresponding expression for the three media (two boundary) system is

$$r_{123} = \frac{r_{12} + r_{23}e^{2ikd}}{1 + r_{12}r_{23}e^{2ikd}},$$

where $k = 2\pi/\lambda$ is the wave vector at the frequency of interest, and r_{12} and r_{23} are the amplitude reflection coefficients at the first and second boundaries, respectively. Finally, this process can be applied recursively to determine the reflectivity from any number of boundaries with arbitrary spacings. To illustrate the process, consider a four medium system in which the distances between the three boundaries are d_1 and d_2. The total amplitude reflectivity, r_{1234}, is given by

$$r_{1234} = \frac{r_{12} + r_{234}e^{2ikd_1}}{1 + r_{12}r_{234}e^{2ikd_1}},$$

where r_{234} is given by

$$r_{234} = \frac{r_{23} + r_{34}e^{2ikd_2}}{1 + r_{23}r_{34}e^{2ikd_2}}.$$

This recursive procedure can be easily programmed to calculate the amplitude reflectivity for any number of boundaries. The absolute squared magnitude of the amplitude reflectivity, r, is the intensity reflectivity, R. Because there is no loss in this simple model, the intensity transmission, T, is simply $1-R$. As we demonstrate in Sec. IV, the theoretical calculations of the gap and defect frequencies made with this model are generally in excellent agreement with the experimentally measured transmission data. It should be noted that there are many methods to calculate the response of a periodic system (Refs. 13 and 15, and references therein). The iterative method described here offers two particular advantages: (i) the method does not invoke Bloch wave propagation so that it can be equally well applied to random or aperiodic systems and (ii) the calculation of effective reflectivities at the interfaces bounding each waveguide segment means that it is possible to determine the longitudinal mode profile within each segment.

III. EXPERIMENTAL CONFIGURATION AND PROCEDURE

The experimental configuration is shown schematically in Fig. 1. The basic experiment consisted of sending an acoustic impulse through a one-dimensional periodic waveguide array and recording the transmitted signal. A numerical Fourier transform of the recorded time-domain signal was used to determine the frequency-dependent transfer function of the sample. The pulse was numerically generated in MATLAB and saved as a standard computer sound file (.wav format). The functional shape of the pulse was chosen to be the second derivative of a Gaussian with a time duration of about 20 ms such that the Fourier transform contained significant frequency components up to 2200 Hz. The form of the pulse was selected because it contained the appropriate spread of frequencies in the range we wished to consider, and it was readily reproducible by the speaker. It should be noted that in addition to the impulse response method we also repeated many of the experiments using a spectrum analyzer and a white noise source. The results with the spectrum analyzer were essentially identical to those obtained with the impulse method.

The time-domain signal used in the data analysis was not due to a single pulse, but rather was the result of a sequence of (typically) 50 pulses that were recorded and averaged. The purpose of this add-and-average procedure was to

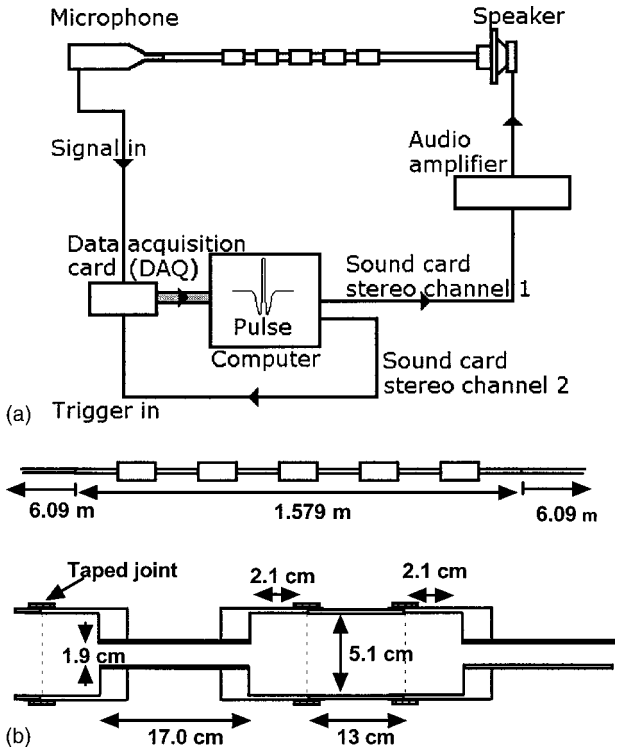

FIG. 1. (a) Schematic representation of the experimental configuration. (b) Schematic representation of the nine-element, diameter-modulated array showing the dimensions.

acquire time-domain data with a high signal-to-noise ratio. The method works because signals reaching the microphone from the speaker added coherently whereas random background noise was quickly averaged out. Because of multiple scattering within the periodic array and from the ends of the sample, some sound persists in the waveguide array for a long time after the initial impulse. To eliminate this long-lived signal we found that, for our particular waveguide parameters, a 7 s delay between successive pulses was required to eliminate interference due to coherent reflections. The validity of this add-and-average method at reducing signal noise can be observed from the initial flat response of the time domain data before the impulse showing that any background sound from previous pulses has been greatly attenuated.

The waveguide structure consisted of three sections of polyvinyl chloride (PVC) pipe being connected, with the speaker at one end and the microphone at the opposite end as shown in Fig. 1(a). The two outer sections of the structure were 6.096 m in length with a diameter of 1.9 cm. The interchangeable middle section contained the diameter-modulated array, which will be described in detail shortly. Each section of pipe was then attached to the adjacent one with masking tape to secure the connection. We found that the use of interlocking PVC pipe connectors to join the sections resulted in backreflections due to the small gap between adjacent pipes within the connectors. The acoustic impedance change due to these gaps led to reflection of the acoustic waves. Although weak, these backreflections were noticeable in the time-domain data. The use of masking tape to join the sections greatly reduced this effect.

At the speaker end, an adapter was constructed to efficiently couple the sound from the speaker to the waveguide. The adapter consisted of a 6-mm-thick piece of Plexiglas™ bolted to the speaker with a 2.0 cm hole centered directly in front of the speaker cone. A 5.1–1.9 cm PVC connector was then attached to the Plexiglas surface. This allowed the unobstructed acoustic impulse from the speaker to be transmitted to the structure. With the adapter in place, there was a distance of 3.8 cm between the cone of the speaker and the waveguide. A pliable foam insulator was then wrapped around the speaker and adapter to reduce the amount of sound emitted into the room.

The microphone was then inserted into the opposite end of the waveguide to a depth of 5.7 cm and was similarly wrapped with a pliable foam insulator. This isolated it from any room reflections that may have been caused by the speaker's initial impulse.

The sequence of events in a typical experiment was as follows. The numerically generated impulse sound file was played through the computer's audio card. The mono wav file was split into the two stereo channels such that each contained an identical version of the pulse. The first channel was sent through the amplifier (Technics model SU-V66) to the speaker (Optimus model number 40-1030, max power 80 W, 8 Ω nominal impedance). The speaker then transmitted the acoustic impulse, which traversed the structure and was received by the microphone (Brüel & Kjaer type 2215 precision sound level meter/octave analyzer). The microphone's signal was then digitized and stored by the data acquisition card (National Instruments PCI 6034E) as shown in Fig. 1(a). The second channel was sent directly to the data acquisition card to act as a trigger to initiate the recording of data. Accurate registration between the trigger and the audio pulse was crucial to the success of the add-and-average process. The sound file of the impulse signal was played by an audio program that looped the sound file so that it repeated at 7 s intervals.

Two acoustic filter structures with different physical parameters were tested. Each structure consisted of a sequence of alternating sections of different diameter PVC pipes. The first experiments used 1.9- and 5.1-cm-diam pipes for the nine-element array as shown in Fig. 1(b). The pipes were cut such that the periodicity of the system was 17.5 cm (distance between changes in cross-sectional area). To couple the two pipes with differing diameters, it was necessary to use 5.1–1.9 cm interlocking PVC pipe adapters. The adapters consisted of essentially two parts, a 5.1-cm-diam part and a 1.9-cm-diam part. The 5.1-cm-diam part of the adapter added a length of 2.1 cm, whereas the 1.9-cm-diam part of the adapter added a length of 0.2 cm. The 5.1-cm-diam pipes were cut to a length of 13.5 cm, and the 1.9-cm-diam pipes were cut to a length of 17.0 cm. Thus, the actual lengths of the sections of pipe were 17.7 cm for the 5.1-cm-diam section and 17.4 cm for the 1.9-cm-diam section. The total length of the periodic array was measured to be 157.9 cm. There was a discrepancy of 0.2 cm throughout the entire length of the array due to minor fabrication and cutting errors in the individual pipe sections. A 1.9 cm straight pipe of identical length was also cut and studied for comparison. The

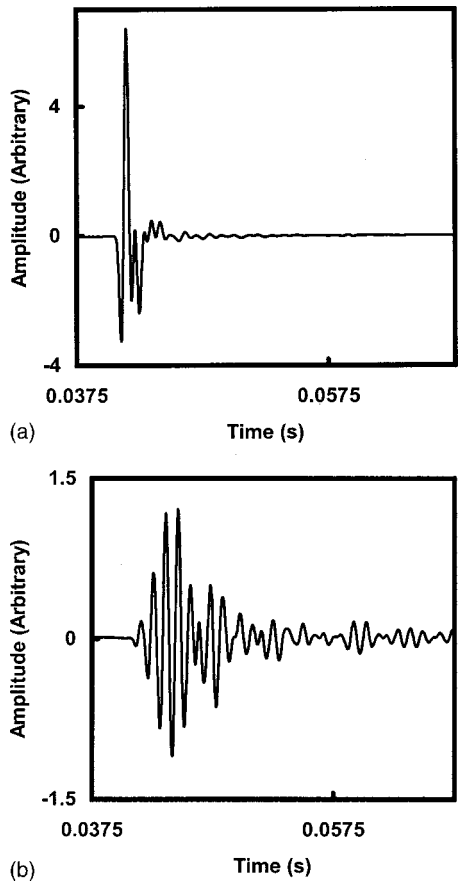

FIG. 2. The transmitted time-domain data obtained for a pulse sent through (a) the straight pipe structure and (b) the nine-element, 1.9- to 5.1-cm-diam modulated waveguide.

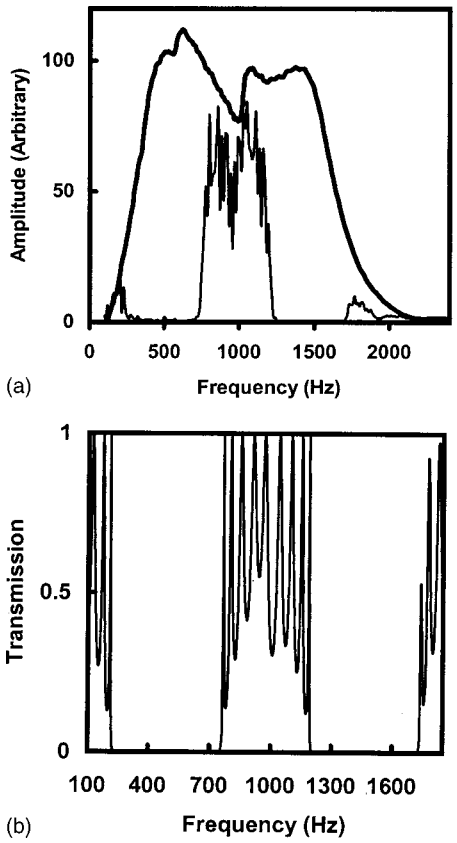

FIG. 3. (a) Composite of the Fourier spectra obtained from the pulses corresponding to Fig. 2(a) (upper dark line) and Fig. 2(b) (lower dark line). (b) Theoretical calculations showing the transmission of the perfectly periodic system.

second acoustic filter structure was similar in construction but with 3.2-cm-diam rather than 5.1-cm-diam segments.

IV. RESULTS AND DISCUSSION

Figures 2(a) and (b) show the transmitted time-domain data obtained from the straight pipe structure and the 1.9- to 5.1-cm-diam modulated waveguide, respectively. The oscillations after the initial pulse in Fig. 2(a) are primarily due to ringing in the speaker and adapter. In Fig. 2(b), the strong extended oscillations after the initial pulse are the result of multiple reflections within the periodic array.

Figure 3(a) is a composite figure of the frequency-domain data obtained from a numerical Fourier transform of the time-domain data for the unobstructed pulse without the array (upper dark line) and the pulse that traversed the diameter-modulated array (lower dark line). By comparing the curves, it can be seen that there are band gaps from 230 to 720 and 1200 to 1700 Hz. This matches closely with the predicted band gaps of 230–720 and 1200–1730 Hz from theoretical calculations as shown in Fig. 3(b).

Next, we altered the array to induce a defect state that would allow an extremely narrow band of frequencies to exist within a band gap. To do this, we modified the length of the middle pipe (5.1 cm diameter) within the nine-element array [see Fig. 1(b)]. We then repeated the above-outlined experimental procedure with middle pipes of various lengths. The frequency-domain data were then obtained from the Fourier transform of these time-domain data. Defect states deep within the band gap region are shown in Fig. 4 for four such structures. Theoretical calculations predict the existence of these modes; however, they predict very narrow (<1 Hz) transmission bands with peaks that ride to a transmission value of 1. One drawback to the narrowness of these defect states is that any minor flaw within the diameter-modulated waveguide will cause the defect states to be greatly attenuated. Inconsistencies within the segment lengths or cross sections of the diameter-modulated waveguide perturb the interference condition and cause slightly different frequencies to pass through the different parts of the waveguide. By the time the pulse gets through the array, very little of the amplitude of the defect frequencies will have added coherently throughout the entire waveguide. For this reason, the second acoustic filter structure with a lower impedance contrast was built. In a sample with a lower impedance contrast, theory predicts defect modes that are less narrow.

With a smaller change in acoustic impedance between adjacent segments, the band gaps become less pronounced and the defect modes become slightly wider. This allows for the coherent addition of a larger group of frequencies within the band gap and thus, greater transmission. Figure 5(a) shows experimental data for two such defect modes within the 1.9- to 3.2-cm-diam modulated waveguide. Figure 5(b) shows a theoretical calculation for the same system indicating that the theory replicates the defect frequencies with high accuracy.

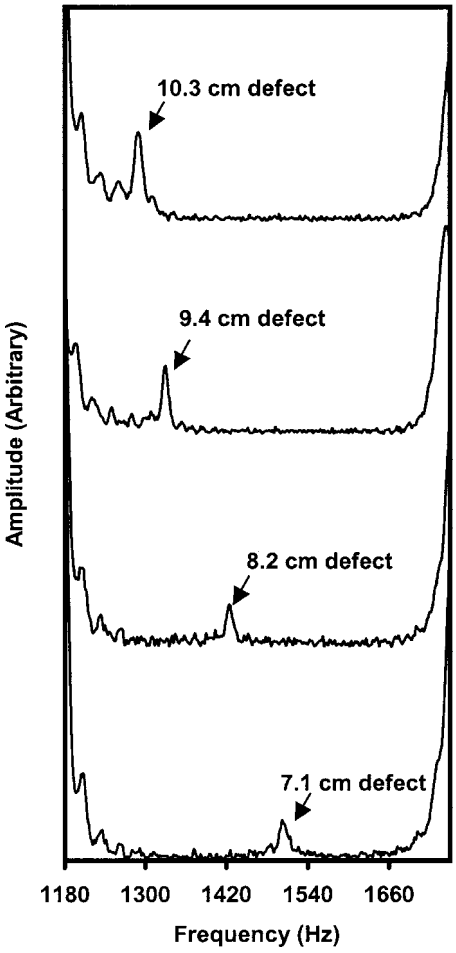

FIG. 4. Composite figure showing the Fourier spectra obtained from four different defects. Data were obtained from the nine-element, 1.9- to 5.1-cm-diam modulated waveguide with middle defects of length 7.1, 8.2, 9.4, and 10.3 cm.

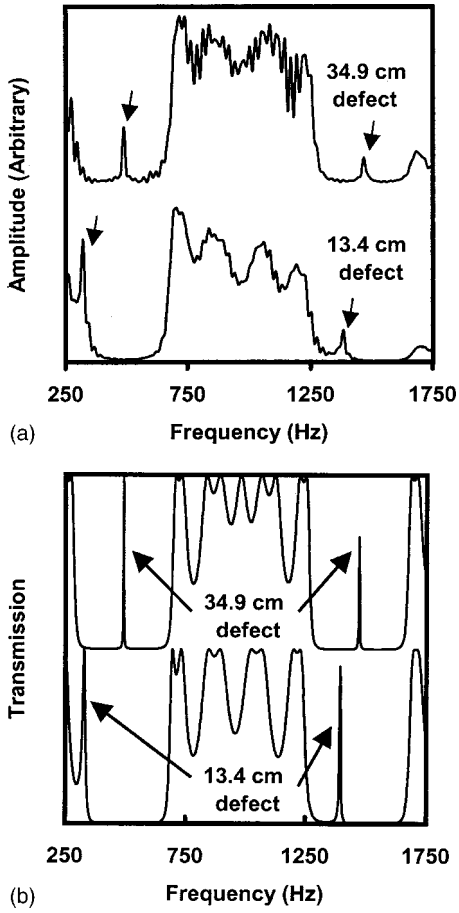

FIG. 5. (a) Composite figure of the Fourier spectra data obtained from the nine-element, 1.9- to 3.2-cm-diam modulated waveguide with middle defects of length 13.4 and 34.9 cm. Defect mode frequencies 489, 1465 Hz (top trace) and 322, 1385 Hz (bottom trace). (b) Theoretical calculations corresponding to the two defect modes in (a). Defect mode frequencies 491, 1474 Hz (top trace) and 326, 1395 Hz (bottom trace).

There are several interesting observations to make concerning the behavior of the defect modes within the band gap. When the induced defect in the middle pipe is shorter than its counterpart in the diameter-modulated array, the defect state in the frequency-domain data enters from the low-frequency side of the band gap (acceptor-like in solid state terms). As shorter defect pipes are used, the defect state moves from low to higher frequency within the band gap. For a defect pipe that is exactly one-half the length of the original pipe within the array, the defect mode appears directly in the middle of the band gap. When larger defect pipes are used, the defect mode enters from the high frequency side of the band gap (donor-like) and moves to lower frequency with increasing length. When the length is exactly double the length of the original pipe within the array, the defect mode again appears directly in the middle of the band gap.

These results can be qualitatively understood by analyzing the physical mechanism that leads to filtering action in these structures. For an array with no defect there is a maximum in reflection (and a corresponding minimum in transmission) at a frequency for which the length of individual array segments equal a quarter wavelength. The enhanced reflection results from constructive interference of the waves partially reflected from each successive junction between array elements of different diameters. For wavelengths that exactly match the quarter-wavelength condition, the successive partial reflections are always precisely in phase because of the combined effects of the half-wavelength round trip between junctions and the inversion upon reflection from a low-to-high impedance junction. The attenuation is a maximum for the design wavelength; however, there is significant filtering action over a broader band of surrounding frequencies leading to the band gap. Now if a defect is introduced by making the center element of the array twice as long, the interference dynamic is altered. The partial reflections from successive interfaces up to the defect are adding coherently to give rise to a strong backreflection. However, the addition of an extra half-wavelength round trip introduced by the defect means that the partial reflections from subsequent half of the array are out of phase resulting in destructive interference in the reflected signal. The net effect is that a narrow transmission band—the defect state—opens up precisely at the design wavelength. Altering the length of the defect will change the wavelength that experiences the half wavelength phase shift and hence will shift the position of the narrow transmission band within the band gap.

It is also interesting to note how the amplitude of the

defect mode varies with position within the band gap. As the defect mode moves deeper into the gap, the amplitude of the defect mode becomes increasingly attenuated. This effect is independent of which side of the band gap the defect mode enters. This phenomenon is similar to that seen in optical filters, and it can be understood because the attenuation is greatest at the center of the band gap where the quarter-wavelength interference condition is best satisfied. The defect in the center of the band is thus strongly confined spatially and therefore very narrow in frequency. Again, any imperfections in the segment lengths or cross-sectional uniformity lead to changes in coupling frequency, which dramatically alter the coupling to the very narrow defect mode. Thus the amplitude of the experimentally measured defect modes is smallest near the band center where the mode confinement is the greatest and progressively larger with proximity to the band edges.

V. CONCLUSION

The results presented here show that the diameter-modulated waveguide array is a simple yet elegant model for investigating acoustic band gap properties. Other similar one-dimensional systems based on dangling side branch arrays have been investigated recently.[11,20] Although the dangling side branch systems are simple experimentally they are less easy to treat theoretically because, unlike the circular cross section waveguide case, there is no simple expression for the acoustic impedance, which in this case depends on frequency.[19] Much of the interesting applications of acoustic band gap systems are associated with the production of defect states in an otherwise perfectly periodic array. The results here demonstrate the experimental limits that prevent the realization of some of the more extreme predictions of theory. Better results could be realized by a more accurate fabrication of the diameter modulated waveguide.

Finally, this simple system should prove useful for the experimental exploration of many of the fundamental effects such as tunneling and localization that are being investigated in acoustic band gap systems.

ACKNOWLEDGMENTS

This work was funded in part by NSF Grant No. ECS-9988797. C.B.B. was supported by a summer research grant from the McNair program.

[1] R. F. Cregan, B. J. Mangan, J. C. Knight, T. A. Birks, P. S. Russell, P. J. Roberts, and D. C. Allan, ''Single-mode photonic band gap guidance of light in air,'' Science **285**, 1537–1539 (1999).
[2] J. C. Chen, H. A. Haus, S. Fan, P. R. Villeneuve, and J. D. Joannopoulos, ''Optical filters from photonic band gap air bridges,'' J. Lightwave Technol. **14**, 2575–2580 (1996).
[3] S. Y. Lin, E. Chow, V. Hietala, P. R. Villeneuve, and J. D. Joannopoulos, ''Experimental demonstration of guiding and bending of electromagnetic waves in a photonic crystal,'' Science **282**, 274–276 (1998).
[4] E. Yablonovitch, ''Inhibited spontaneous emission in solid state physics and electronics,'' Phys. Rev. Lett. **58**, 2059–2062 (1987).
[5] M. S. Kushwaha, P. Halevi, L. Dobrzynski, and B. Djafari-Rouhani, ''Acoustic band structure of periodic elastic composites,'' Phys. Rev. Lett. **71**, 2022–2025 (1993).
[6] Z. Ye and E. Hoskinson, ''Band gaps and localization in acoustic propagation in water with air cylinders,'' Appl. Phys. Lett. **77**, 4428–4430 (2000).
[7] A. Diez, G. Kakarantzas, T. A. Birks, and P. St. J. Russell, ''Photonic stop bands in optical fibre periodic microstructures,'' Appl. Phys. Lett. **76**, 3481–3483 (2000).
[8] W. M. Robertson and J. F. Rudy, ''Measurement of acoustic stop bands in two-dimensional periodic scattering arrays,'' J. Acoust. Soc. Am. **104**, 694–699 (1998).
[9] J. V. Sanchez, D. Caballero, R. Martinez-Sala, J. Sancho, C. Rubio, J. Sanchez-Dehesa, F. Meseguer, J. Llinares, and F. Galvez, ''Sound attenuation by two dimensional array of rigid cylinders,'' Phys. Rev. Lett. **80**, 5325–5328 (1998).
[10] B. Djafari-Rouhani, J. O. Vasseur, A. Akjouj, L. Dobryznski, M. S. Kushwaha, P. A. Deymer, and J. Zemmouri, ''Giant stop bands and defect modes in one-dimensional waveguide with dangling side branches,'' Prog. Surf. Sci. **59**, 255–264 (1998).
[11] M. S. Kushwaha, A. Akjouj, B. Djafari-Rouhani, L. Dobrzynski, and J. O. Vasseur, ''Acoustic spectral gaps and discrete transmission in slender tubes,'' Solid State Commun. **106**, 659–663 (1998).
[12] W. P. Mason, *Electromechanical Transducers and Wave Filters* (Van Nostrand, Princeton, 1948), pp. 28–31.
[13] C. E. Bradley, ''Time harmonic acoustic Bloch wave propagation in periodic waveguides. I. Theory,'' J. Acoust. Soc. Am. **96**, 1844–1853 (1994).
[14] C. E. Bradley, ''Time harmonic acoustic Bloch wave propagation in periodic waveguides. II. Experiment,'' J. Acoust. Soc. Am. **96**, 1854–1862 (1994).
[15] R. S. Langley, ''The frequency band-averaged wave transmission coefficient of a periodic structure,'' J. Acoust. Soc. Am. **100**, 304–311 (1996).
[16] R. S. Langley, ''Wave transmission through one-dimensional near periodic structures: Optimum and random disorder,'' J. Sound Vib. **188**, 717–743 (1995).
[17] T. D. Rossing, ''Experiments with an impedance tube in the acoustics laboratory,'' Am. J. Phys. **50**, 1137–1141 (1982).
[18] P. M. Morse, *Vibration and Sound* (McGraw–Hill, New York, 1936), Chap 7.
[19] L. E. Kinsler, A. R. Frey, A. J. Coppens, and J. V. Sanders, *Fundamentals of Acoustics* (Wiley, New York, 1982).
[20] J. Ash and W. M. Robertson, ''Breaking the sound barrier: Tunneling of acoustic pulses through the forbidden transmission region of a one-dimensional acoustic band gap array,'' Am. J. Phys. **70**, 689–693 (2002).